HHS Public Access

Author manuscript

Technol Cancer Res Treat. Author manuscript; available in PMC 2016 July 21.

Published in final edited form as:

Technol Cancer Res Treat. 2016 June ; 15(3): 460–471. doi:10.1177/1533034615584522.

Adaptation, Commissioning, and Evaluation of a 3D Treatment Planning System for High-Resolution Small-Animal Irradiation

Jeho Jeong, PhD[1], **Qing Chen, MS**[1], **Robert Febo, BS**[1], **Jie Yang, PhD**[1], **Hai Pham, MS**[1], **Jian-Ping Xiong, MS**[1], **Pat B. Zanzonico, PhD**[1], **Joseph O. Deasy, PhD**[1], **John L. Humm, PhD**[1], and **Gig S. Mageras, PhD**[1]

[1] Department of Medical Physics, Memorial Sloan-Kettering Cancer Center, New York, NY, USA

Abstract

Although spatially precise systems are now available for small-animal irradiations, there are currently limited software tools available for treatment planning for such irradiations. We report on the adaptation, commissioning, and evaluation of a 3-dimensional treatment planning system for use with a small-animal irradiation system. The 225-kV X-ray beam of the X-RAD 225Cx microirradiator (Precision X-Ray) was commissioned using both ion-chamber and radiochromic film for 10 different collimators ranging in field size from 1 mm in diameter to 40 × 40 mm^2. A clinical 3-dimensional treatment planning system (Metropolis) developed at our institution was adapted to small-animal irradiation by making it compatible with the dimensions of mice and rats, modeling the microirradiator beam orientations and collimators, and incorporating the measured beam data for dose calculation. Dose calculations in Metropolis were verified by comparison with measurements in phantoms. Treatment plans for irradiation of a tumor-bearing mouse were generated with both the Metropolis and the vendor-supplied software. The calculated beam-on times and the plan evaluation tools were compared. The dose rate at the central axis ranges from 74 to 365 cGy/min depending on the collimator size. Doses calculated with Metropolis agreed with phantom measurements within 3% for all collimators. The beam-on times calculated by Metropolis and the vendor-supplied software agreed within 1% at the isocenter. The modified 3-dimensional treatment planning system provides better visualization of the relationship between the X-ray beams and the small-animal anatomy as well as more complete dosimetric information on target tissues and organs at risk. It thereby enhances the potential of image-guided microirradiator systems for evaluation of dose–response relationships and for preclinical experimentation generally.

Corresponding Author: John L. Humm, PhD, Department of Medical Physics, Memorial Sloan-Kettering Cancer Center, 1275 York Ave, New York, NY 10065, USA. hummj@mskcc.org.

1. D_{95}: the dose covering 95% of the volumes; D_{05}: the dose covering 5% of the volumes; and D_{mean}: mean dose.

Declaration of Conflicting Interests

The author(s) declared no potential conflicts of interest with respect to the research, authorship, and/or publication of this article.

Supplemental Material

The online data supplements are available at http://tct.sagepub.com/supplemental.

Keywords

small-animal irradiator; radiation therapy; commissioning; treatment planning system; 3D dose distribution

Introduction

Preclinical animal experimentation has been an essential tool in evaluating the effectiveness of anticancer therapies, studying the underlying mechanisms of disease response, and providing evidence of safety for new drugs and devices.[1] In radiotherapy and radiobiology research, preclinical experimentation has long been used to investigate the response of tumor or normal tissue to radiation exposure, usually with small animals such as mice and rats. Although there are, of course, some differences between such animal models and humans,[2] their genomic similarities result in generally comparable radiation response and cell kinetics, thus allowing translation of information drawn from small-animal experiments to clinical treatment techniques for patients with cancer.[3,4]

For the study of small animals, microimaging tools, which are customized to generate high-resolution images, have been developed. These scaled-down imaging modalities, such as micropositron emission tomography (micro-PET),[5] microcomputed tomography (micro-CT),[6,7] micromagnetic resonance imaging (micro-MRI),[8] and microsingle-photon emission CT (micro-SPECT),[9] have played an important role in preclinical research.

In contrast, irradiation systems used in small-animal research have been less advanced relative to microimaging tools. Until recently, nonconformal irradiation of small-animal tumors and organs has usually been performed with large-field irradiators and manual collimation with lead shielding and without accurate dose calculation, which is markedly different from clinical practice. Many tumor response studies were thus hampered by nonuniform and otherwise suboptimal tumor irradiation and by prohibitive normal tissue complications and ensuing mortality, which could be mitigated by reducing the unnecessary dose to normal tissues.[10] Also, the recent emergence of more clinically realistic transgenic and other orthotopic tumor models in small animals, rather than subcutaneous and other superficial xenograft models, requires precise depth-dose information with image guidance.

To overcome these problems, small-animal image-guided irradiation systems have been developed by several institutions, including Princess Margaret Hospital,[11,12] Johns Hopkins University,[13,14] Stanford University,[15-17] and Washington University in St Louis.[18] These irradiation systems have been scaled down both in geometry and energy in order to be compatible with small-animal dimensions. Due to the difficulty in reliably positioning a small animal during setup for irradiation,[19] image guidance is necessary, and most of the microirradiators that have been developed use on-board conebeam CT.

Our institution purchased and installed the X-RAD 225Cx, a small-animal irradiator with CT image-guidance capability that was based on the design developed by Princess Margaret Hospital and commercialized by Precision X-ray (North Branford, Connecticut) for advanced preclinical radiotherapy research. However, the software supplied by the vendor

for programming small-animal irradiations provides the absorbed dose at a specified target point but does not provide capabilities for complex treatment planning, specifically, graphical tools for specifying the arrangement of radiation beams, visualizing the relationship of the beams to the animal anatomy using 3-dimensional (3D) images, accurate calculation of the radiation dose distribution and its visualization on the 3D images, and derivation of dose-volume histograms (DVHs) for tumor or other target structures and organs at risk.

Thus, the rationale of our study is to enhance an image-guided small-animal irradiation system with advanced treatment planning capabilities equivalent to those used in patients and to thereby allow clinically translatable preclinical radiotherapy hypothesis testing in experimental animal tumor models. This article describes the adaptation, commissioning, and evaluation of a 3D treatment planning system (TPS) with such capabilities for use with an X-RAD 225Cx microirradiator system, with a brief description of the irradiator itself.

Methods

Small-Animal Irradiator

The X-RAD 225Cx (Precision X-ray Inc) small-animal irradiator, with image-guidance capability, was used. With an X-ray tube equipped with 2 different focal spot sizes (1- or 5 mm diameter), the tube potential of the irradiator is adjustable from 20 to 225 kV. The system also provides a high-resolution conebeam CT image, using a 20 × 20-cm^2 amorphous silicon digital X-ray detector (1024 × 1024 pixels with dynamic imaging capability up to 15 frames per second) with a 360° gantry rotation (maximum speed of 3 rpm) about a specified isocenter.

The X-RAD 225Cx is operated in either an imaging or an irradiation mode. In the imaging mode, the X-ray tube potential is normally set between 40 and 120 kV, with anode currents between 0.5 and 3 mA. The small focal spot (1 mm) and 2-mm aluminum filter are used, and the scan time is about 60 seconds. In the irradiation mode, the typical X-ray tube potential is 225 kV, with a 13-mA current, large focal spot (5 mm), and 0.3-mm copper filter. The system is equipped with 10 different collimators, which provide different irradiation field sizes that range from a circular collimator with a diameter (φ) of 1 mm to a square collimator providing a 40 × 40-mm^2 irradiation field. The specimen stage of the microirradiator is capable of moving in 3 orthogonal directions (x, y, and z) with a positional accuracy of less than 0.1 mm and crossed laser beams provide direct visualization of the position of the isocenter. The system is self-shielded in a cabinet (88 in h × 72 in w × 48 in d) with radiation leakage that is less than 1 μSv/h at a distance of 10 cm from the cabinet surface. More detailed information about the system has been published.[10-12]

Irradiator Beam Commissioning

The irradiator was commissioned for a typical irradiation setting at 225 kV and 13 mA. For the 10 different collimators, the absorbed dose at the isocenter was measured with varying depths in a solid-water phantom. Before the measurement, the laser-based isocenter of the beam was verified. A small ball bearing was carefully placed at the laser-based isocenter,

and fluoroscopic images were acquired as the gantry was rotating around the isocenter (Supplemental Figure 1). The laser-based isocenter was verified to be stable, and all of the following measurements were performed at the laser-visualized isocenter.

Both ion-chamber and radiochromic film (EBT3; Ashland Inc, Wayne, New Jersey) were used for beam commissioning. Due to the small field size, a compact ion chamber with a 0.04-cm^3 active volume (CC04; IBA Dosimetry, Bartlett, Tennessee) was used for the measurement. However, for field sizes smaller than 10 mm in diameter, only radiochromic film measurements were performed because the active volume of CC04 is still prohibitively large for reliable dose measurements. For measurements at or near the surface, a parallel-plate chamber (LXPC-6D; MSKCC, New York, NY, USA) was used. The CC04 and parallel-plate chambers were cross-calibrated, based on the Farmer chamber (Exradin A12; Standard Imaging, Middleton, Wisconsin) calibrated by the National Institute of Standards and Technology. In-air measurements of each chamber were compared for the beam at 225 kV and 13 mA with a 40 × 40 mm^2 collimator. Due to the small field size and short source-detector distance available in the microirradiator, the recommendations of TG-61[20] could not be directly applied. According to our dose measurement protocol, the absorbed dose was determined using Farmer chamber. From the chamber reading, the exposure rate was acquired, and then the exposure-to-dose conversion factor was applied along with the temperature/pressure correction and electrometer correction. Comparing the readings of CC04 and parallel-plate chambers with the dose determined by Farmer chamber, dose-conversion factors for the CC04 and parallel-plate chambers were derived.

The half-value layer (HVL) for the X-RAD 225Cx's irradiation-mode settings (225 kV, 13 mA, large 5-mm focal spot, and 0.3-mm copper filter) was measured with the CC04 ion chamber in the air with additional copper filters of various thicknesses. To reduce scatter from the X-ray head, the ion chamber was placed far below the laser-based isocenter, and the position of the chamber was adjusted so as to be at the center of the field, based on fluoroscopic imaging. The set-up is shown in Supplemental Figure 2. The active volume of the CC04 chamber was placed at a distance of 28.8 cm up to the collimator's aperture and 8.3 cm down to the detector's cover. The additional copper filters were placed on a stand at a distance of 1.5 cm from the collimator's aperture.

The HVL was measured for 2 different collimators (40 × 40 mm^2 and 20 × 20 mm^2), and the first and second HVLs were estimated by the interpolation of the 2 measurements on either side of the HVLs, based on the following equation[21]:

$$HVL = \left\{ (T_2 - T_1) \times \frac{ln\,(I_0/2) - ln\,I_1}{ln\,I_2 - ln\,I_1} \right\} + T_1 \quad (1)$$

where I_0 is the dose measured without an additional copper filter; I_1 and I_2 are the doses measured on either side of the HVL; and T_1 and T_2 are the corresponding thicknesses of the additional copper filters for I_1 and I_2, respectively.

Before measurement of the absorbed dose with EBT3 radiochromic film, calibration of the film is required. Film calibration was performed based on the absolute doses measured with

the ion chamber for several time intervals. Both the ion-chamber and EBT3 films were irradiated under the same conditions, with a 40 × 40-mm^2 collimator at a depth of 2 cm in the solid-water phantom. A calibration curve was generated by correlating the ion-chamber measurement with the film's optical density. The films were scanned with an EPSON expression 10000XL scanner (EPSON America Inc., Long Beach, CA, USA), and FilmQA pro software (Ashland Inc) was used for calibration and further dose analysis.

For measurement of the absorbed dose, films were placed at the laser-based isocenter under the solid-water phantom and measurements were made at 8 different depths in the phantom (from the surface to 50 mm). An additional 50-mm thickness of solid-water phantoms was placed below the film for backscatter. For the 10 different collimators, this procedure was repeated with varying irradiation times that were increased for the smaller collimators to compensate for the lower dose rate provided by the smaller collimators.

The exposed films were stored in dark conditions for about a day for fixation and the next day scanned 1 film at a time with the EPSON expression 10000XL scanner. For different collimator sizes, the following different scan resolutions were used: a 72 dots per inch (dpi) resolution was used for larger collimators (40 × 40 mm^2, 20 × 20 mm^2, φ25 mm, and φ15 mm), 150 dpi for 10 × 10 mm^2 and φ10 mm, and 200 dpi for smaller collimators (φf5, φ3.5, φ2.5, and φ1 mm). Using the FilmQA pro software and the previously derived calibration curve, 2D dose maps of each collimator were acquired for various depths. This procedure is summarized in Supplemental Figure 3.

To verify the doses measured by EBT3 film, the absolute dose was measured using cross-calibrated CC04 and parallel-plate ion chambers. For 3 collimators (40 × 40 mm^2, 10 × 10 mm^2, and φ10 mm), the absorbed doses were measured at the central axis of the beam with the CC04 chamber in the water-equivalent solid phantom (Supplemental Figure 4a). The chamber was placed at the laser-based isocenter within the solid-water phantom, and the measurements were made at 9 different thicknesses of the solid-water phantom (from 1 to 5 cm in increments of 0.5 cm), with an additional 5-cm thickness of solid-water placed below the chamber for backscatter.

Since the dose at depths less than 10 mm cannot be measured with the CC04 chamber within the solid-water phantom, the parallel-plate chamber was used to measure doses at or near the surface. For 4 different collimators (40 × 40 mm^2, 20 × 20 mm^2, φ25 mm, and φ15 mm), the field size is larger than the active volume of the parallel-plate chamber (~ 11.3-mm diameter), and the absorbed dose was measured in a combination of the water-equivalent solid phantom and polystyrene phantom (Supplemental Figure 4b).

For collimators with a field size smaller than the active volume of both ion chambers (φ5, φ3.5, φ2.5, and φ1 mm), the dose cannot be properly measured with the ion chambers and therefore these measurements were not performed.

Treatment Planning System

The Memorial Treatment Planning System (Metropolis) is the latest version of the external-beam radiation TPS developed at our institution (although we have now adopted a

commercial system for clinical applications). It is designed to run on multicore workstations with the Windows operating system. Treatment planning data are stored in a relational database (Microsoft SQL Server), with binary large object data (eg, images and deformation vector fields) stored on shared network drives. The dose calculation algorithm in Metropolis is based on the former version of TPS that has been published elsewhere.[22-25]

Metropolis uses a graphical user interface and includes the following capabilities: display of 3D image sets (CT, MRI, and PET) in transverse, coronal, sagittal, and 3D surface views; rigid and deformable registration and fusion of 3D image sets; manual and semiautomatic tools for image segmentation; specification of the arrangement of radiation beams and visualization of beam intersection with the patient anatomy; beam's eye-view (BEV); generation of digitally reconstructed radiographs (DRRs) for treatment verification; design of static field and 3D conformal fields treatment plans; visualization of dose distributions on the 3D images; and generation of DVHs.

Modifications were made to Metropolis to adapt it to treatment planning with the small-animal irradiator. The image display zoom function and precision of delineated volumes and DVHs were adjusted to be compatible with small-animal sizes. Selectable kilovoltage X-ray beam energies and associated collimators (from 1-mm diameter circular to 40 × 40 mm^2 square fields) were added and graphically overlaid in the BEV, 2D, and 3D image displays. To achieve appropriate spatial resolution for volume dose calculation and DVHs, the calculation grid spacing was reduced to 0.1 mm. The default calculation grid is 0.2 mm, which is the same as the CBCT pixel resolution. The 0.1 mm calculation grid is used when higher resolution is desired, for example, when planning with the 1 mm diameter beam collimator. The dose calculation formalism was adapted to film dosimetry-based commissioning and predefined collimators, as described further subsequently. There are other available features of Metropolis such as optimization of intensity modulated radiation therapy (IMRT) plans and generation of dynamic multileaf collimator sequences for IMRT delivery that could not be utilized at this time because of the absence of a multileaf collimator in the small-animal irradiation system.

Dose Calculation of Irradiated Fields

Dose calculation in Metropolis is based on commissioned beam output data. The dose to each voxel is calculated by the summation of each beam dose:

$$D(x,y,d) = T \times \dot{D}(d) \times OCR(x,y,d) \times G \quad (2)$$

where T is the beam-on time, $\dot{D}(d)$ is the central axis dose rate at isocenter and depth d, OCR(x, y, d) is the off-center ratio (OCR) at position (x, y) from the central axis as measured on a plane through the isocenter and normal to the central axis, and G is the inverse square factor. Coordinates (x, y) are determined by the intersection of the ray from the X-ray source to the dose calculation point within the isocenter plane. The depth is calculated assuming homogeneous water-equivalent density within the body surface. The dose rate and OCR can be directly obtained from EBT3 film measurements for the 10

different collimators. For depths at which the film measurement was not performed, the dose was estimated by the interpolation of 2 bracketing measurements.

To import the film measurement into Metropolis, the 2D dose maps of the film were rotated to match the collimator angle, and the center of the field was determined by finding the midline between the edges at half-maximum intensity. The dose map was also smoothed based on its nearest neighbors, while preserving the penumbra.

Validation of Metropolis Dose Calculation

The dose calculation in Metropolis was validated by comparing the calculated dose with the dose measured in the phantom (Supplemental Figure 5). For all 10 collimators, the central axis dose at a 20-mm depth in the phantom for an irradiation time of 1 min was calculated in Metropolis, based on CT images of a stack of solid-water phantoms. The actual dose was measured with EBT3 film at the same depth (20 mm) in between the slabs of solid-water and then compared with the calculated dose.

Comparison of Metropolis and the Vendor-Supplied Software

The Metropolis software tools for treatment planning were evaluated and compared with the vendor-supplied software for the X-RAD 225Cx. Starting from a 3D CT image, an example plan was generated in each system to treat a tumor in the shoulder of a mouse with 2 orthogonal beams, each prescribed to deliver 2 Gy to the isocenter.

In the vendor-supplied software, a treatment isocenter was selected on a single CT transverse slice, 2 beams were defined and collimators selected based on tumor size on the CT images. The isocenter depth for each beam was computed from a body contour determined by image thresholding on the selected CT slice. The beam-on time was calculated based on the depth dose of each beam (Figure 1).

In Metropolis, 3D structures (body surface, tumor, and lung) were delineated on the stack of CT transverse images (Figure 2a). Isocenter placement and beam collimation were defined based on tumor volume coverage on BEV display (Figure 2b). Three-dimensional dose calculation was performed, and the plan was evaluated based on dose distributions overlaid on the CT images and DVHs.

Results

Half-Value Layer

The HVL measured for the typical beam output of the X-RAD 225Cx microirradiator (225 kV and 13 mA) was almost the same for 2 different collimator sizes (40×40 mm^2 and 20×20 mm^2), as shown in Supplemental Figure 6. The first HVL was estimated to be 0.91 mm and the second HVL 1.93 mm, which yielded the homogeneity coefficient of .47 for the beam.

Dose Linearity and Timer Error

For film calibration, the absorbed dose was measured at various irradiation times, using the cross-calibrated CC04 chamber within the solid-water phantom with a 40 × 40-mm^2 collimator. As shown in Supplemental Figure 7, the dose was proportional to the irradiation time, with a coefficient of determination (R^2) value of 1.0. From the plot (Supplemental Figure 7), the x-axis intercept of the linear regression line could also be used to estimate the irradiator's on–off (or timer) error, which was evaluated to be approximately 0.4 second.

Calibration Curve for EBT3 Film

A calibration curve was generated for the EBT3 film by correlating the optical density of the film with the absorbed dose (measured with the CC04 chamber, Supplemental Figure 7). As shown in Supplemental Figure 8, the optical density of the film increased (the film became darker) as the irradiation time increased, and the calibration curve could be found as a rational function for each of the 3-color channels (red, green, and blue). Among the 3, the red channel was used for calibration, since it provided the greatest dynamic range for the measured dose range.

Dose Rate Measured With EBT3 Film

The dose rates measured on the central axis for the 10 different collimators at various depths are shown in Table 1 and Figure 3. The surface measurement was excluded, since the film measurement seemed to underestimate the surface dose when compared with the parallel-plate chamber measurement (see Comparison between ion-chambers and EBT3 section for more details). For the largest (40 × 40 mm^2) collimator, the maximum dose rate was found to be approximately 365 cGy/min at a depth of 1 mm. The dose rate decreased as the beam size (area of the field) decreased. Compared with the largest collimator, the dose rate with the smallest collimator (φ1 mm) decreased by more than a factor of 2. As depth increased in the phantom, the dose rate decreased. For smaller collimators, the dose decreased more sharply with increase in depth due to less scatter, as shown in Supplemental Figure 9.

In addition to the central axis dose, the EBT3 film provides 2D dose distribution for the entire radiation field, as shown in Supplemental Figure 10 for 2 collimators at a depth of 1 mm. From the 2D dose map, a dose profile can be acquired for any axis. In Supplemental Figures 11 to 13, the horizontal and vertical dose profiles at the central axis are shown for all 10 collimators at various depths in the solid-water phantom. In Figure 4, the horizontal (the transverse axis for the animal) dose profiles are compared for all the collimators at a depth of 20 mm. The overall dose rate decreased for smaller collimators. For this depth (20 mm), the dose decreased laterally with distance from the central axis, due to the longer transmission length in the phantom and less scatter. The out-of-field dose increased with field size. The larger collimators (40 × 40 mm^2 and φ25 mm) exhibit asymmetry in the horizontal profile (arrows in Supplemental Figures 11 and 13), probably due to the inhomogeneous field of the X-ray or misalignment of the collimator, as discussed by Lindsay et al.[26]

Comparison Between Ion Chambers and EBT3

The doses on the beam central axis were measured for several collimators with 2 different types of ion chambers (CC04: 40 × 40 mm^2, 20 × 20 mm^2, and φ10 mm; LXPC-6D: 40 × 40 mm^2, 20 × 20 mm^2, φ25 mm, and φ15 mm), as shown in Supplemental Tables 1 and 2. The absolute doses measured from the ion chambers were compared with the EBT3 film measurements. For the 40 × 40-mm^2 collimator, for which 3 measurements were performed, the comparison is shown in Figure 5. Except for the surface measurement (comparison between LXPC-6D and EBT3), all 3 measurements agreed, within a difference of 3%.

The discrepancy in surface dose measurements is possibly caused by the 120-μm-thick transparent polyester substrate covering the active layer of EBT3 film. Therefore, the surface measurement made with EBT3 film was discarded. In Supplemental Figures 14 and 15, the comparison between EBT3 film and each ion chamber is shown for other collimators. As the collimator size decreased and the depth in phantom increased, the discrepancy between film and ion-chamber measurements increased, presumably because the ion-chamber measurement provides the average dose over the active volume. For smaller collimators at depth, the ion-chamber measurement might underestimate the actual dose at the central axis.

Verification of Dose Calculation in Metropolis

To verify the dose calculation in Metropolis, the dose measured at a depth of 20 mm in the solid-water phantom was compared with that calculated with Metropolis. For all 10 collimators, the differences in dose rate were less than 3%, as shown in Table 2. The calculated dose was consistently lower than the measured dose, which might have been caused by smoothing of the 2D dose map while importing the film measurement into Metropolis. The dose profiles calculated in Metropolis were also compared with the measured profiles for a square collimator (10 × 10 mm^2) and a circular collimator (φ10 mm) at 3 depths (5, 20, and 40 mm). As shown in Supplemental Figure 16, the profiles agree to each other within 3.3% difference for the whole range.

Comparison of Metropolis Versus Vendor-Supplied Software

The calculated beam-on times for the 2 TPSs are shown in Table 3 and agree within 1%. In addition to the beam-on-time calculation, Metropolis provides 3D plan evaluation tools. Using 3D isodose distribution, as shown in Figure 6, the coverage of the target and fall-off of dose outside the target can be evaluated. Also, using the DVH functionality (Figure 6), quantitative evaluation of treatment plans is possible and reveals tumor dose variation (D_{95}: 388 cGy; D_{05}: 401 cGy) and dose to lung (D_{mean}: 84 cGy) for a prescribed isocenter dose of 400 cGy (note 1).

Discussion

The beam quality of the X-RAD 225Cx microirradiator was evaluated for typical irradiation settings of 225 kV and 13 mA, for which the HVL was 0.91 mm Cu with a homogeneity coefficient of .47. The dose rate for the largest area collimator (40 × 40 mm^2) was about 3.6 Gy/min at a depth of 1 mm. The dose rate decreased as the collimator size decreased and depth in a solid-water phantom increased. Except for the smallest area (1 mm) circular

collimator at a depth greater than 30 mm, the dose rate was higher than 1 Gy/min, below which the cell repair mechanism during irradiation can become an issue.[27,28] Beam output is very stable during irradiation. The delivered dose was linear with irradiation time ($R^2 \approx 1.0$), with a small timer error of about 0.4 second, which can be ignored for most applications.

The commissioned beam data were compared with other institutional data of the same system (X-RAD 225Cx). The depth dose curves and dose profiles along the horizontal axis were compared with the multi-institutional data published by Lindsay et al,[26] as shown in Supplemental Figures 17 and 18. Although the dose profiles were comparable to other institutional data, the depth doses were considerably higher than others, which might be caused by the differences in the X-ray tube and generator used in our institution. The multi-institutional microirradiators use MXR-225/22 X-ray tube with GE Isovolt 225 Titan generator, while our unit uses MXR-225/26 tube (COMET, Flamatt, Switzerland) with GE Isovolt Titan E generator (GE Sensing & Inspection Technologies, Ahrensburg, Germany). The difference might also result in slightly larger timer error of 0.4 second, compared to the reported 0.2 second in their units.

The Metropolis dose calculation algorithm appears to have adequate accuracy for small-animal irradiations, as verified in the comparison between the measured dose in phantom and the dose calculated in Metropolis (Table 2 and Supplemental Figure 16). However, heterogeneity correction is currently not available in Metropolis without CT number calibration for the 225-kV energy beam, and bone perturbations, in particular, can be challenging. For convex geometry, the dose calculation may overestimate the actual dose, because it is based on dose measurement in a large solid-water phantom (20×20 cm^2). Monte Carlo calculation can overcome this geometric limitation and increase dose calculation accuracy.[29] Metropolis currently has a Monte Carlo dose calculation algorithm, but it is optimized for clinical use with megavoltage beams. Future plans are to commission it for kilovoltage X-ray beams and the microirradiator geometry.

Metropolis uses the CT image transferred from the X-RAD software in standard DICOM format. To validate the imported CT image as well as the DRR generation in Metropolis, DRRs were generated and compared with the orthogonal radiographic images taken for the same mouse in the same position, as shown in Supplemental Figure 19. Although quantitative comparison is difficult due to the quite different image quality without the adjustment of level and window settings, the bones and soft tissue visualized in DRRs are comparable with the radiographic images, which validates the CT image transfer and DRR generation.

Metropolis provides excellent tools for treatment planning and analysis, including various tools for contouring and 3D dose evaluation. With Metropolis, the dose to the targets and normal tissues can be preevaluated, and the plan can be modified if the dose distribution is unsatisfactory. The conformity of dose to the target structures can be evaluated by analyzing the isodose distribution and DVHs, and the isocenter placement, beam arrangement and weighting, and choice of collimators can be adjusted to improve conformity. Moreover, the

dose to normal tissue can be reduced, thereby reducing toxicity and morbidity and increasing the survival of the animal and the quality of the experiment.

An example is shown in Figure 7 for a mouse having 2 orthotopic mammary tumors on both sides of the abdomen. The mouse was treated with 12 Gy at the center of each tumor with the φ15 mm collimator using the vendor-supplied software. For the treatment verification, 3 different plans were developed in Metropolis and compared afterward (plan 1: 2 vertical beams with the φ15 mm collimator for both tumors; plan 2: 2-angled beams based on BEV with the φ15 mm collimator; and plan 3: 2-angled beams based on BEV with 20 × 20 mm^2 collimator).

When the beam angles were adjusted based on the BEV (plan 2), the normal tissue sparing was substantially improved while maintaining the same tumor dose. The spinal cord maximum dose was decreased by a factor of 10 compared to plan 1 (D_{max}: 99.6 vs 1039 cGy; D_{mean}: 48.5 vs 270 cGy). The dose to other normal tissues (all structures excluding tumors and spinal cord) was also decreased (D_{mean}: 221 vs 279 cGy). For both plans with the φ15 mm collimator (plans 1 and 2), however, the tumors were not fully covered as shown in the BEVs (Figure 7A and B), which implies underirradiation of the tumor edge (D_{min} for plan 1: 216 and 95.3 cGy for left and right tumors, respectively; D_{min} for plan 2: 471 and 120 cGy for left and right tumors, respectively).

To improve tumor coverage, another plan with the 20 × 20 mm^2 collimator (plan 3) was formulated. As shown in the DVH (Figure 7C), the target coverage improved without unirradiated areas (D_{min}: 1056 and 1086 cGy for left and right tumors, respectively). Due to the larger field size, the dose to the normal tissues increased, although the does to spinal cord remained comparable to that in plan 2. The comparison of DVHs is available in Supplemental Figure 20 and the dose distribution parameters were compared in Supplemental Table 3.

The general experiment workflow using either vendor-supplied TPS or Metropolis is shown in Supplemental Figure 21. Despite many advantages, the treatment planning procedure in Metropolis requires more time, mainly due to the 3D structure definition (contouring) procedure, while the procedure in the vendor-supplied software defines a single body surface contour on a single CT slice and is therefore simpler and requires less time. For rapid planning of straightforward irradiations, the vendor-supplied software should suffice. However, when comprehensive analysis is required (eg, with a radiosensitive normal tissue structure adjacent to or impinging on a targeted tumor), Metropolis can be invaluable, using stored CT images and treatment plan information (including the treatment isocenter, collimator size, beam angles, and beam-on times), as shown in the previous example.

After we implemented Metropolis for the use with the microirradiator, the vendor released another commercially available TPS, called SmART-Plan.[30] Developed in collaboration with the MAASTRO Clinic, the software provides similar tools for treatment planning of small animals. Compared to that software, Metropolis has advantages in that the dose calculation algorithm was commissioned based on the beam data of our own microirradiator and

provides greater flexibility with various built-in tools, including Monte Carlo dose calculation algorithm and multimodality image registration.

Because the use of a microirradiator involves guidance with CT, radiographic, or fluoroscopic imaging, the dose from the imaging mode was also evaluated, using ion chamber and optically stimulated luminescence (OSL) dosimetry. The dose rates for several typical tube voltages and current settings were evaluated, as shown in Supplemental Figure 22. The evaluated dose rates were between approximately 1 and 12 cGy/min, which increased with higher tube voltage and current.

Considering the CT acquisition time is about 1 minute, the dose from 1 CT imaging session is therefore less than 12 cGy. The dose from radiographic and fluoroscopic imaging is dependent on the imaging time, which is usually less than that of CT imaging. This result shows that the dose from modalities used for imaging guidance is not a concern, considering the irradiation dose is usually greater than 10 Gy.

Conclusions

The 225-kV beam of the X-Rad 225Cx small-animal microirradiator was thoroughly commissioned for all collimators. Based on the commissioning data, an in-house 3D TPS, Metropolis, was implemented for the irradiator. Metropolis provides better visualization of the relationship between the X-ray beams and the small-animal anatomy as well as more complete dosimetric information of target tissues and organs at risk, allowing the full potential of advanced microirradiator radiation treatment planning to be conducted for preclinical experimentation. The availability of a 3D TPS is timely given the recent drive in the radiation research community to adopt orthotopic and transgenic animal tumor models that more closely recapitulate human cancer histopathology.

Supplementary Material

Refer to Web version on PubMed Central for supplementary material.

Acknowledgments

The authors thank Thomas LoSasso, PhD, Gary Lim, MS, and Grace Tang, PhD, in the Department of Medical Physics at Memorial Sloan-Kettering Cancer Center for advising and helping with the dosimetric methodology, including film processing, and Brian Quinn, MS, in the Department of Medical Physics at Memorial Sloan-Kettering Cancer Center for checking the leakage dose from the microirradiator and providing OSL dosimeters.

Funding

The author(s) disclosed receipt of the following financial support for the research, authorship, and/or publication of this article: This work was partly supported by a research grant from the Geoffrey Beene Cancer Research Center at Memorial Sloan-Kettering Cancer Center.

Abbreviations

BEV	beam's eye-view
CT	computed tomography

DRR	digitally reconstructed radiograph
DVHs	dose-volume histograms
HVL	half-value layer
IMRT	intensity modulated radiation therapy
MRI	magnetic resonance imaging
OCR	off-center ratio
OSL	optically stimulated luminescence
PET	positron emission tomography
TPS	treatment planning system
3D	3-dimensional

References

1. Martin DS, Balis ME, Fisher B, et al. Role of murine tumor models in cancer treatment research. Cancer Res. 1986; 46(4 pt 2):2189–2192. [PubMed: 3948188]
2. Anisimov VN, Ukraintseva SV, Yashin AI. Cancer in rodents: does it tell us about cancer in humans? Nat Rev Cancer. 2005; 5(10):807–819. [PubMed: 16195752]
3. Kallman RF. Animal experiments in radiotherapy I—small animals. J Can Assoc Radiol. 1975; 26(1):15–24. [PubMed: 1141370]
4. Waterston RH, Lindblad-Toh K, Birney E, et al. Initial sequencing and comparative analysis of the mouse genome. Nature. 2002; 420(6915):520–562. [PubMed: 12466850]
5. Yao R, Lecomte R, Crawford ES. Small-animal PET: what is it, and why do we need it? J Nucl Med Tech. 2012; 40(3):157–165.
6. Badea CT, Drangova M, Holdsworth DW, Johnson GA. In vivo small-animal imaging using micro-CT and digital subtraction angiography. Phys Med Biol. 2008; 53(19):R319–R350. [PubMed: 18758005]
7. Schambach SJ, Bag S, Schilling L, Groden C, Brockmann MA. Application of micro-CT in small animal imaging. Methods. 2010; 50(1):2–13. [PubMed: 19706326]
8. Lee SC, Kim K, Kim J, et al. One micrometer resolution NMR microscopy. J Magn Reson. 2001; 150(2):207–213. [PubMed: 11384182]
9. Golestani R, Wu C, Tio RA, et al. Small-animal SPECT and SPECT/CT: application in cardiovascular research. Eur J Nucl Med Mol Imaging. 2010; 37(9):1766–1777. [PubMed: 20069298]
10. Verhaegen F, Granton P, Tryggestad E. Small animal radiotherapy research platforms. Phys Med Biol. 2011; 56(12):R55–R83. [PubMed: 21617291]
11. Clarkson R, Lindsay PE, Ansell S, et al. Characterization of image quality and image-guidance performance of a preclinical micro-irradiator. Med Phys. 2011; 38(2):845–856. [PubMed: 21452722]
12. Newton J, Oldham M, Thomas A, et al. Commissioning a small-field biological irradiator using point, 2D, and 3D dosimetry techniques. Med Phys. 2011; 38(12):6754–6762. [PubMed: 22149857]
13. Matinfar M, Gray O, Iordachita I, et al. Small animal radiation research platform: imaging, mechanics, control and calibration. Med Image Comput Comput Assist Interv. 2007; 10(pt 2):926–934. [PubMed: 18044657]

14. Deng H, Kennedy CW, Armour E, et al. The small-animal radiation research platform (SARRP): dosimetry of a focused lens system. Phys Med Biol. 2007; 52(10):2729–2740. [PubMed: 17473348]
15. Graves EE, Zhou H, Chatterjee R, et al. Design and evaluation of a variable aperture collimator for conformal radiotherapy of small animals using a microCT scanner. Med Phys. 2007; 34(11):4359–4367. [PubMed: 18072501]
16. Bazalova M, Zhou H, Keall PJ, Graves EE. Kilovoltage beam Monte Carlo dose calculations in submillimeter voxels for small animal radiotherapy. Med Phys. 2009; 36(11):4991–4999. [PubMed: 19994508]
17. Zhou H, Rodriguez M, van den Haak F, et al. Development of a micro-computed tomography–based image-guided conformal radiotherapy system for small animals. Int J Radiat Oncol. 2010; 78(1):297–305.
18. Stojadinovic S, Low DA, Hope AJ, et al. MicroRT-small animal conformal irradiator. Med Phys. 2007; 34(12):4706–4716. [PubMed: 18196798]
19. Armour M, Ford E, Iordachita I, Wong J. CT guidance is needed to achieve reproducible positioning of the mouse head for repeat precision cranial irradiation. Radiat Res. 2010; 173(1): 119–123. [PubMed: 20041766]
20. Ma CM, Coffey CW, DeWerd LA, et al. AAPM protocol for 40-300 kV x-ray beam dosimetry in radiothearpy and radiobiology. Med Phys. 2001; 28(6):868–893. [PubMed: 11439485]
21. Hill AL. Half value layer measurements to facilitate patient dose assessment for newer CT scanners using published normalized dose data. Br J Radiol. 1999; 72(860):792–798. [PubMed: 10624346]
22. Mohan R, Chui C, Lidofsky L. Energy and angular distributions of photons from medical linear accelerators. Med Phys. 1985; 12(5):592–597. [PubMed: 4046993]
23. Chui CS, LoSasso T, Spirou S. Dose calculation for photon beams with intensity modulation generated by dynamic jaw or multileaf collimations. Med Phys. 1994; 21(8):1237–1244. [PubMed: 7799865]
24. Wang X, Spirou S, LoSasso T, Stein J, Chui CS, Mohan B. Dosimetric verification of intensity-modulated fields. Med Phys. 1996; 23(3):317–327. [PubMed: 8815373]
25. Spirou SV, Chui C. A gradient inverse planning algorithm with dose-volume constraints. Med Phys. 1998; 25(3):321–333. [PubMed: 9547499]
26. Lindsay PE, Granton PV, Gasparini A, et al. Multi-institutional dosimetric and geometric commissioning of image-guided small animal irradiators. Med Phys. 2014; 41(3):031714. [PubMed: 24593718]
27. Steel GG, Down JD, Peacock JH, Stephens TC. Dose-rate effects and the repair of radiation damage. Radiother Oncol. 1986; 5(4):321–331. [PubMed: 3726169]
28. Steel GG, Deacon JM, Duchesne GM, Horwich A, Kelland LR, Peacock JH. The dose-rate effect in human tumour cells. Radiother Oncol. 1987; 9(4):299–310. [PubMed: 3317524]
29. Chow JCL, Leung MKK, Lindsay PE, Jaffray DA. Dosimetric variation due to the photon beam energy in the small-animal irradiation: a Monte Carlo study. Med phys. 2010; 37(10):5322–5329. [PubMed: 21089767]
30. van Hoof SJ, Granton PV, Verhaegen F. Development and validation of a treatment planning system for small animal radiotherapy: SmART-Plan. Radiother Oncol. 2013; 109(3):361–366. [PubMed: 24183860]

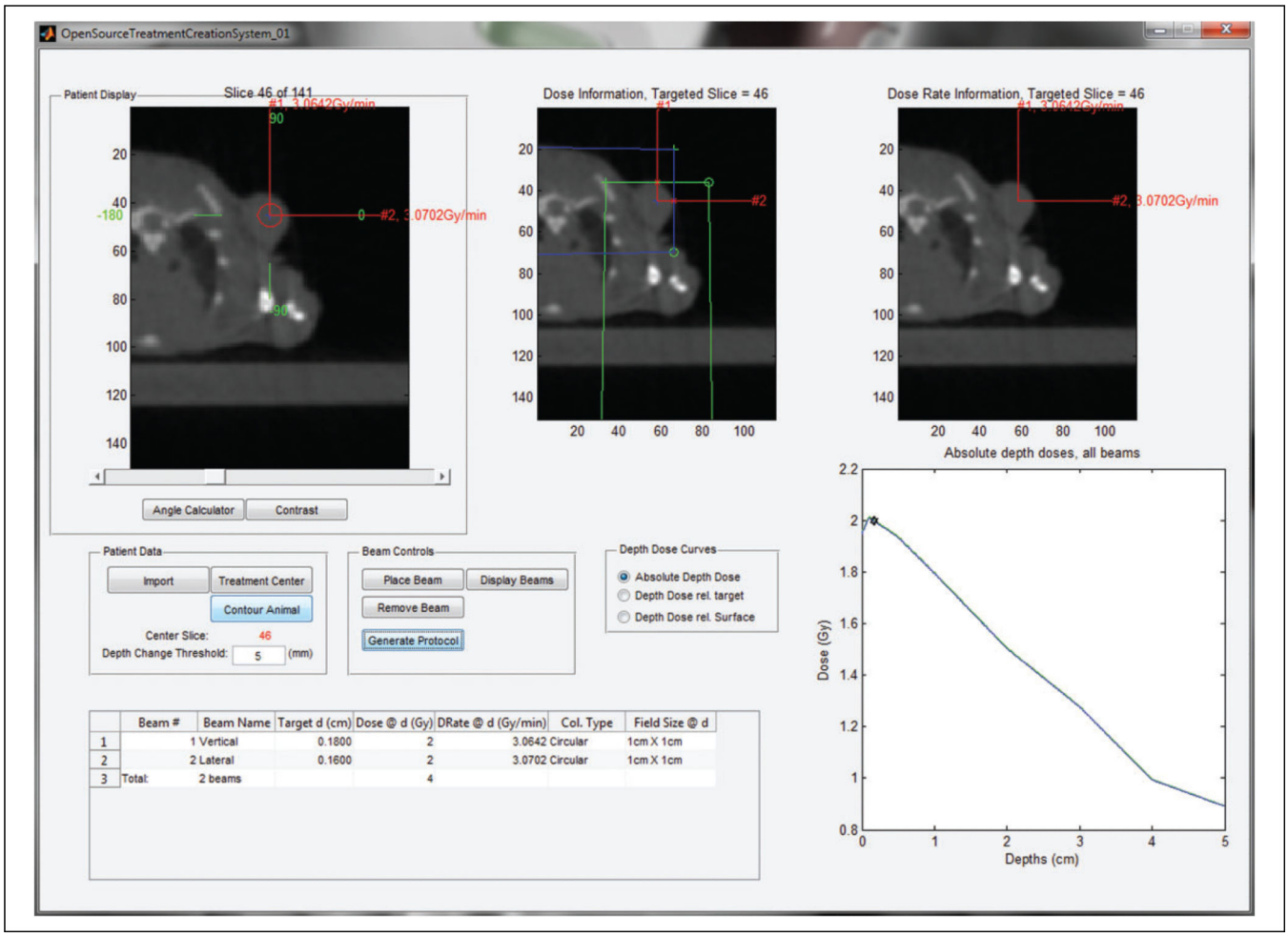

Figure 1.

The interface of the vendor-supplied software, in which the beam-on time can be calculated based on the depth dose for each beam to a treatment isocenter. Note that the longer axial dimension of the tumor (as shown in Figure 2) required the use of the 10-mm circular collimator to assure adequate coverage, even though it unavoidably resulted in including normal tissues in the transaxial directions.

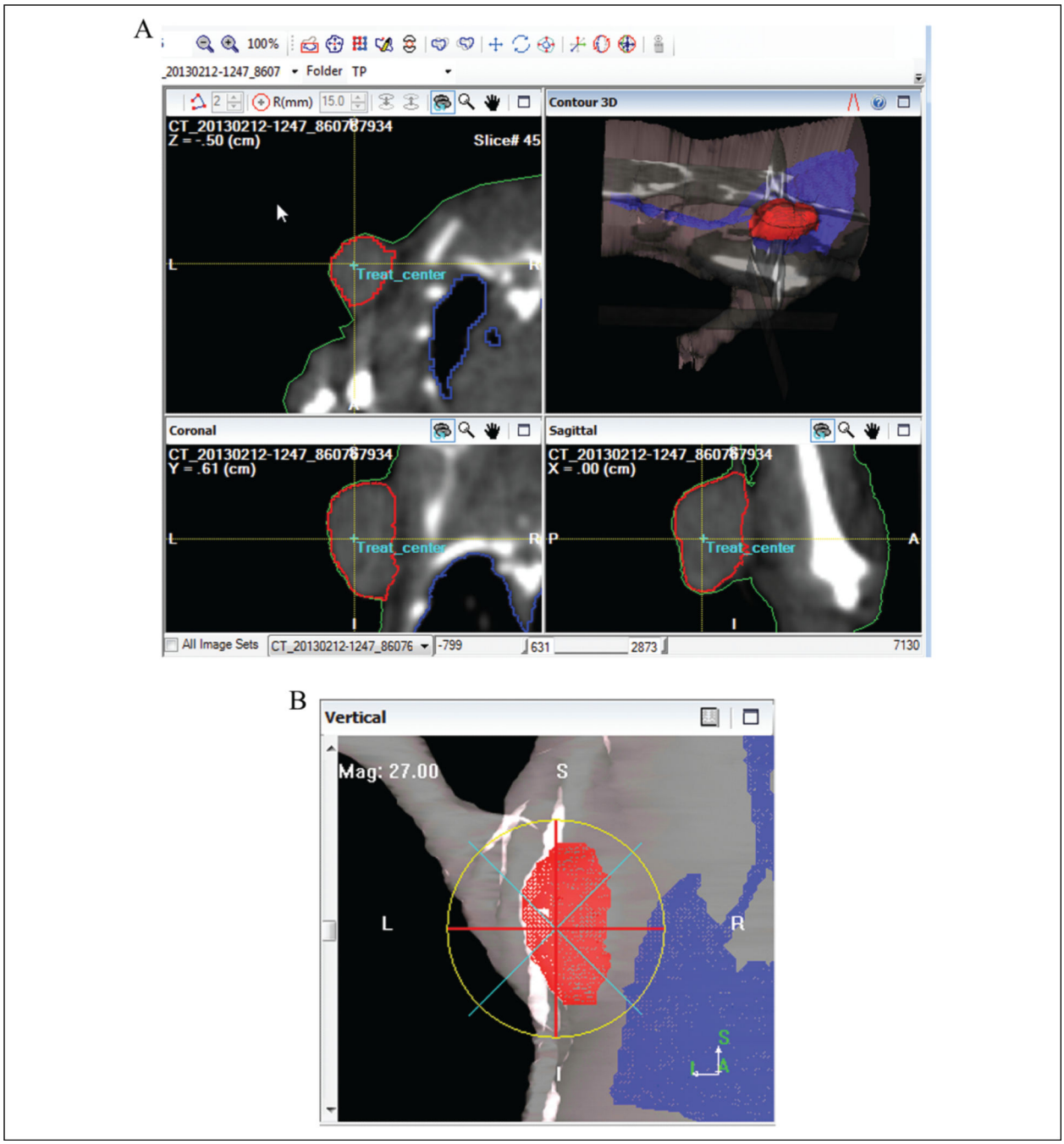

Figure 2.

The interface of Metropolis: (A) segmentation of structures including tumor using contouring tools and (B) beam's eye-view (BEV).

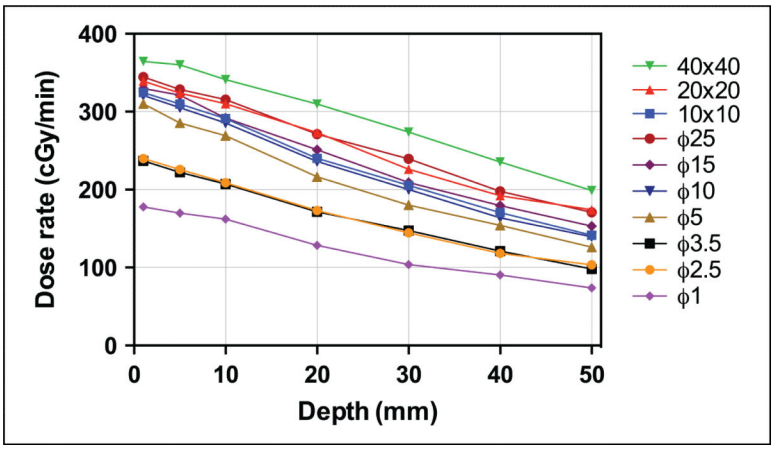

Figure 3.

Dose rate on central axis of the field at varying depths in the solid-water phantom measured by EBT3 film for all 10 collimators. The symbol "φ" refers to the diameter of circular collimators.

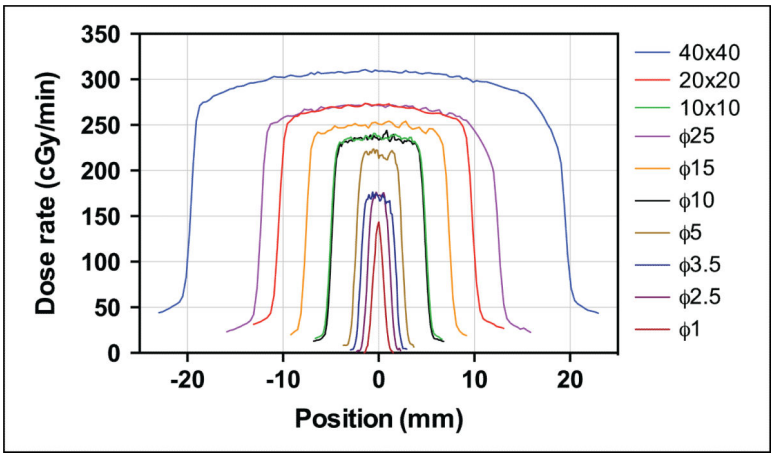

Figure 4.

Horizontal dose profiles measured with EBT3 films at a 20-mm depth in the solid-water phantom for the 10 different collimators (see Supplemental Figures 11-13 for individual profiles for each collimator). The symbol "φ" refers to the diameter of circular collimators.

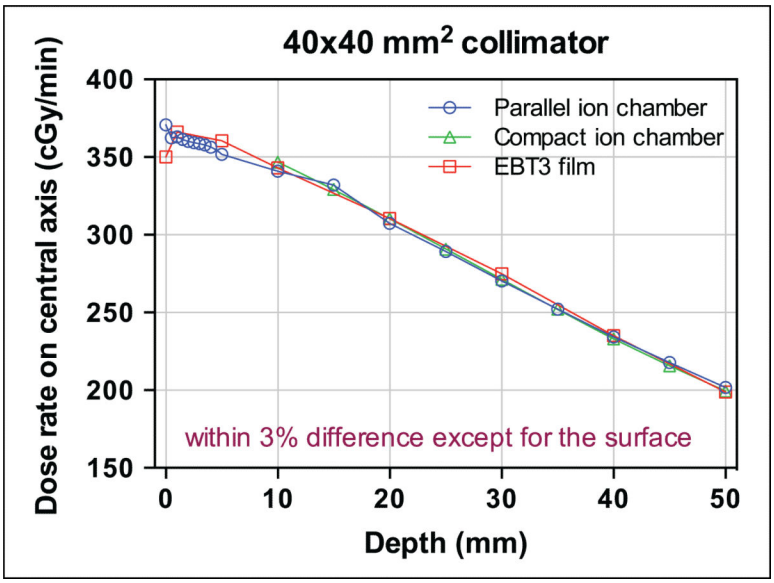

Figure 5.
Comparison of depth-dependent dose rate measured with 3 different dosimeters for a 40 × 40-mm^2 collimator.

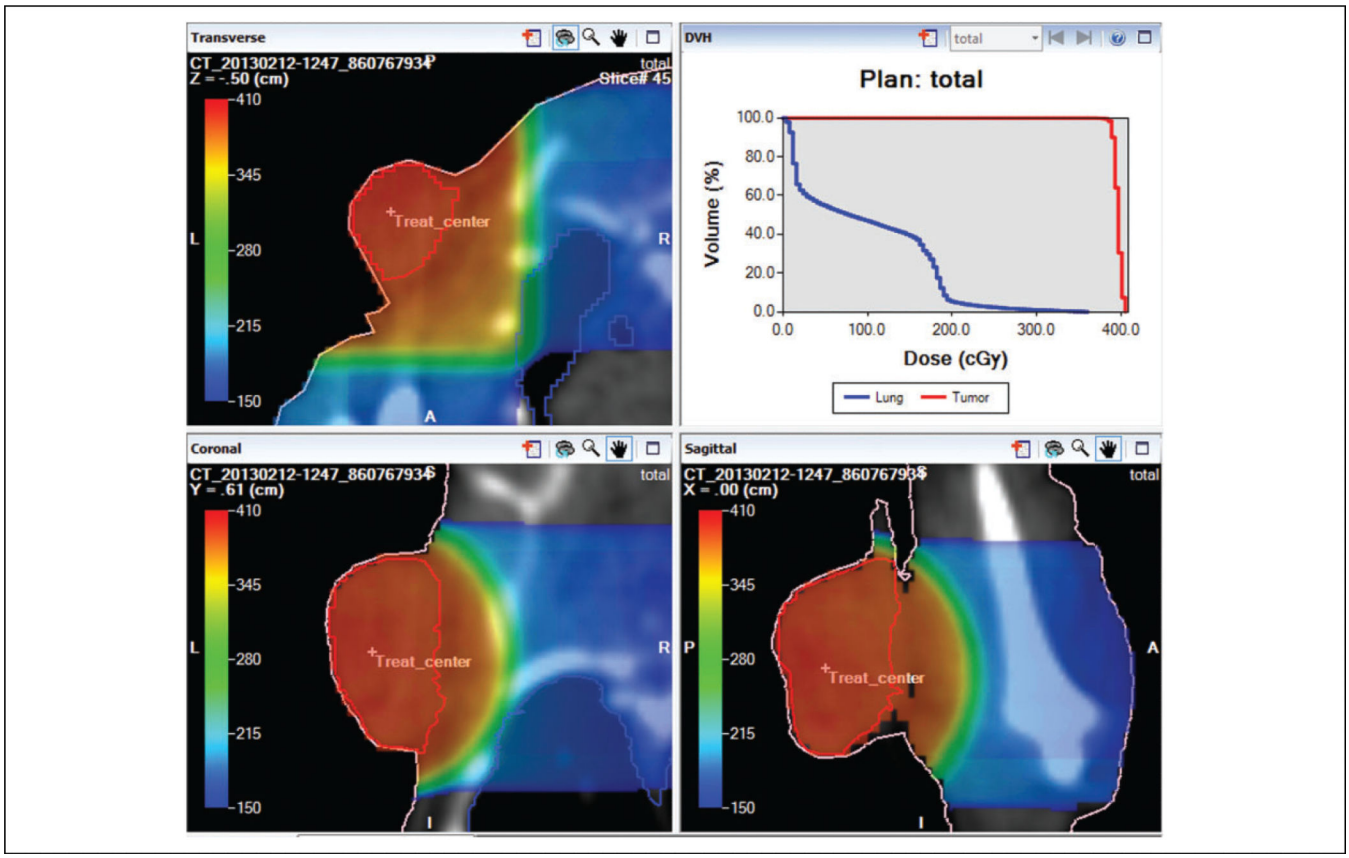

Figure 6.

Plan evaluation in Metropolis with 3-dimensional (3D) isodose distribution (color wash) and dose-volume histograms (DVHs) for 2 orthogonal beams of 10-mm diameter. Red, blue, and pink curves indicate tumor, lung, and body surface in the transverse, coronal, and sagittal view images.

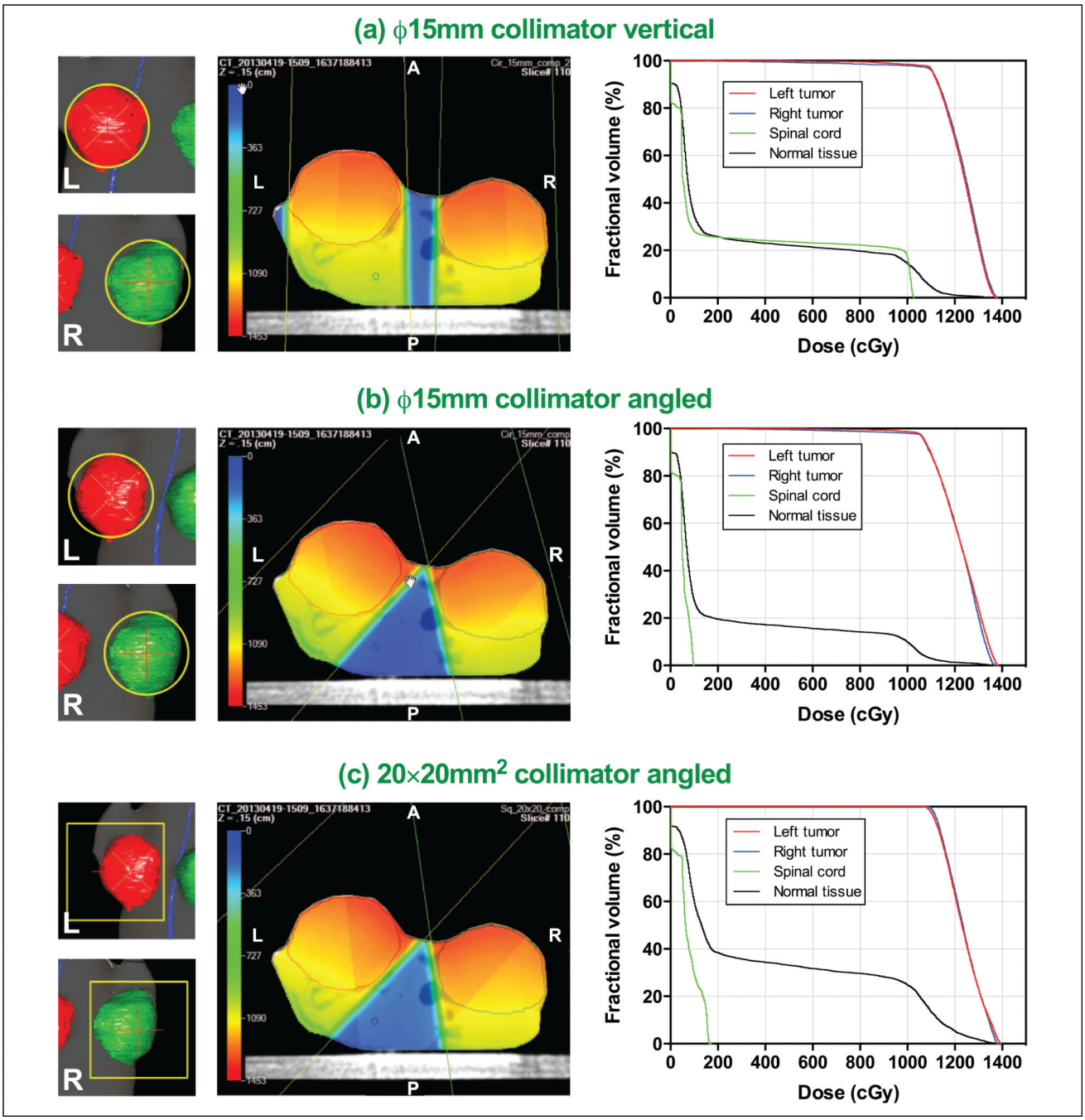

Figure 7.

Comparison of target coverage shown in beam's eye-view (BEV; left column), 3-dimensional (3D) isodose distribution in color-wash overlaid on transverse computed tomography (CT) image (middle column), and dose-volume histogram (DVH; right column) for 3 different plans: (A) 2 vertical beams with φ15 mm collimator, (B) 2 angled beams with φ15 mm collimator for the critical structure (spinal cord), and (C) 2 angled beams with 20 × 20 mm^2 collimator to cover whole targets.

Table 1

Dose Rate on Central Axis of the Field at Varying Depths in the Solid-Water Phantom Measured by EBT3 Film for 10 Collimators.

	Dose Rate on Central Axis, cGy/min									
	Square Collimators, mm^2			Circular Collimators, Diameter in mm						
Depth, mm	**10 × 10**	**20 × 20**	**40 × 40**	**φ1**	**φ2.5**	**φ3.5**	**φ5**	**φ10**	**φ15**	**φ25**
1	324.5	339.2	364.6	177.8	239.8	236.9	310.2	320.9	329.8	344.5
5	309.7	323.7	360.2	169.9	225.7	222.2	285.4	305.3	321.2	328.5
10	291.2	310.3	341.1	162.0	208.7	207.3	269.1	285.4	291.7	315.4
20	240.0	273.2	309.8	128.6	173.1	171.6	216.6	236.2	251.2	271.1
30	205.5	226.1	273.7	103.7	144.6	147.4	180.0	200.1	209.2	239.5
40	170.5	192.2	235.5	90.5	118.2	121.1	154.1	163.8	179.5	197.9
50	141.5	174.0	198.8	73.9	103.4	98.3	126.1	139.6	153.3	170.7

Technol Cancer Res Treat. Author manuscript; available in PMC 2016 July 21.

Table 2

The Dose Difference Between Metropolis Calculation and Film Measurement.

Collimator, mm^2 or mm in Diameter	Dose Rate Measured With EBT3 Film, cGy/min	Dose Rate Calculated in Metropolis, cGy/min	% Difference in Dose
10 × 10	240.0	233.0	–2.9
20 × 20	273.2	267.5	–2.1
40 × 40	309.8	305.6	–1.4
φ1	128.6	126.2	–1.8
φ2.5	173.1	169.2	–2.3
φ3.5	171.6	166.7	–2.8
φ5	216.6	214.6	–0.9
φ10	236.2	232.0	–1.8
φ15	251.2	247.9	–1.3
φ25	271.1	268.0	–1.1

Table 3

Beam-On Times Calculated by 2 Different TPSs for the Vertical and Lateral Beams of the Plan.

	Beam-On Time, Seconds	
TPS	**Vertical**	**Lateral**
Vendor-supplied software	37.9	37.8
Metropolis	37.7	37.7

Abbreviation: TPS, treatment planning system.